ChemistryOpen

Research Article
doi.org/10.1002/open.202100253

Chemistry Europe
European Chemical Societies Publishing

www.chemistryopen.org

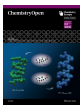

Exploring Helical Folding in Oligomers of Cyclopentane-Based ε-Amino Acids: A Computational Study

Hae Sook Park[b] and Young Kee Kang*[a]

The conformational preferences of oligopeptides of an ε-amino acid (2-((1*R*,3*S*)-3-(aminomethyl)cyclopentyl)acetic acid, Amc_5a) with a cyclopentane substituent in the C^{β}–C^{γ}–C^{δ} sequence of the backbone were investigated using DFT methods in chloroform and water. The most preferred conformation of Amc_5a oligomers (dimer to hexamer) was the H_{16} helical structure both in chloroform and water. Four residues were found to be sufficient to induce a substantial H_{16} helix population in solution. The Amc_5a hexamer adopted a stable left-handed (*M*)-2.3_{16} helical conformation with a rise of 4.8 Å per turn. The hexamer of Ampa (an analogue of Amc_5a with replacing cyclopentane by pyrrolidine) adopted the right-handed mixed (*P*)-$2.9_{18/16}$ helical conformation in chloroform and the (*M*)-2.4_{16} helical conformation in water. Therefore, hexamers of ε-amino acid residues exhibited different preferences of helical structures depending on the substituents in peptide backbone and the solvent polarity as well as the chain length.

Introduction

For two decades, there has been a great advance in the synthesis and structural characterization of various peptide foldamers.[1–9] Peptide foldamers are oligomers of non-natural amino acids that adopt well-defined structural motifs, similar to those of natural peptides and proteins.[1–9] It has been known that oligomers of β-, γ-, or δ-amino acid residues as well as their hybrids with α-amino acid residues can adopt various secondary structures as found in structures of peptides and proteins.[1–9] In particular, peptide foldamers can stabilize various helical structures, of which the type, handedness, and macrodipole direction of helices can be controlled by the substitutions and/or stereochemistry of the residues.[1–20] Helical peptide foldamers have been used to design (a) antimicrobial peptides (AMPs) with cationic groups[3,4,21–24] and (b) catalysts for various organic reactions by incorporating catalytic functional groups.[25–31]

It is well known that the polymer nylon 6 of the ε-amino caproic acid (6-aminohexanoic acid, Ahx; Figure 1a) forms fibrils composed of β-sheet-like chain structures.[32,33] A polymer of ε-L-lysine (2,6-diaminohexanoic acid; Figure 1b) (ε-PL) was first isolated from culture filtrates of *Streptomyces albulus*, which is composed of ~25 lysine residues and exhibits antimicrobial activity against several human microbial pathogens.[34–36] The spectra of far-UV circular dichroism measurements for ε-PL in aggregates supported that ε-PL chains in aqueous solution are rich in β-sheet-like structure even at room temperature.[37] Oligomers of branched ε-L-lysines with pendant α-peptides were suggested as good DNA compaction agents with potential as delivery vectors.[38] However, there has been no report for the synthesis and conformational analysis of peptide foldamers composed of ε-amino acids, probably due to the experimental difficulties in the synthesis and incorporation of chirospecific

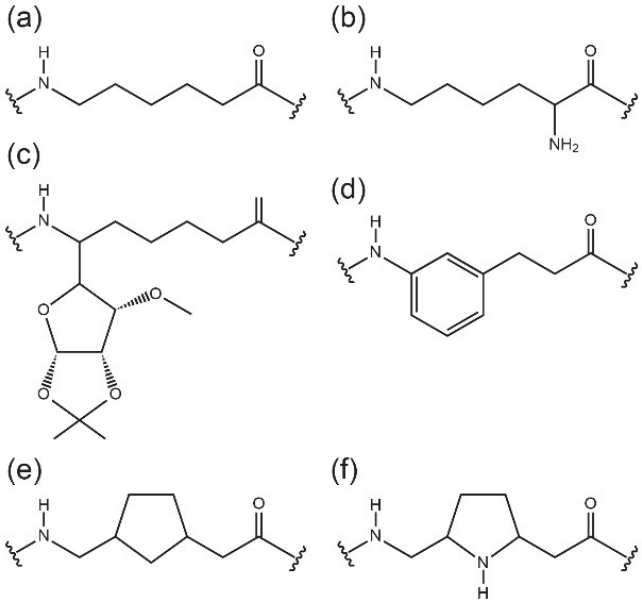

Figure 1. Chemical structures of various ε-amino acid residues reported in the literature: (a) ε-amino caproic acid (6-aminohexanoic acid, Ahx), (b) ε-L-lysine (2,6-diaminohexanoic acid), (c) (*S*)-C-linked carbo-ε-amino acid [(*S*)-ε-$Caa_{(x)}$], (d) 3-(3-aminophenyl)propanoic acid, (e) 2-(3-(aminomethyl)cyclopentyl)acetic acid (Amc_5a; this work), and (f) 2-(5-(aminomethyl)pyrrolidin-2-yl)acetic acid (Ampa; this work).

[a] *Prof. em. Y. K. Kang*
Department of Chemistry
Chungbuk National University, Cheongju
Chungbuk 28644 (Republic of Korea)
E-mail: ykkang@chungbuk.ac.kr
[b] *Prof. Dr. H. S. Park*
Department of Nursing
Cheju Halla University
Cheju 63092 (Republic of Korea)

Supporting information for this article is available on the WWW under https://doi.org/10.1002/open.202100253

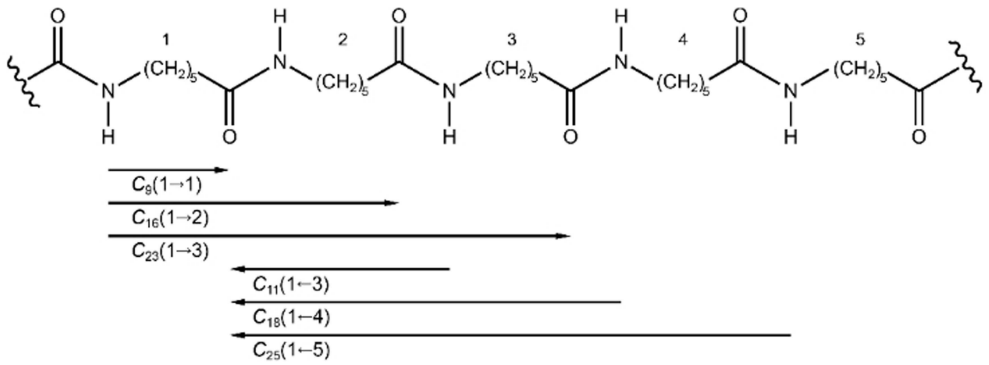

Figure 2. Feasible H-bond types in ε-peptides. C_n denotes the H-bonded pseudocyle with n atoms: C_9, C_{16}, and C_{23} H-bonds in forward direction; C_{11}, C_{18}, and C_{25} H-bonds in backward direction.

building blocks. There are only two reports for the conformational preferences of α/ε-hybrid peptides to date. Sharma et al. designed an α/ε-hybrid hexapeptide containing L-Ala and (*S*)-C-linked carbo-ε-amino acid [(*S*)-ε-Caa$_{(x)}$; Figure 1c] constituents in 1 : 1 alteration and suggested its structure as a novel mixed $H_{14/12}$ helix by ^{1}H NMR experiments.[39] The synthesis and structural characterization of another α/ε-hybrid tetrapeptide composed of Aib and 3-(3-aminophenyl)propanoic acid (Figure 1d) in 1 : 1 alteration were reported by Haldar and his co-workers.[40] Temperature-dependent ^{1}H NMR experiments of the α/ε-hybrid tetrapeptide supported the formation of a ribbon-like structure in $CDCl_3$.

Only limited works studied by quantum-mechanical methods have focused on the conformational preferences of ε-peptides. Computational studies using density functional theory (DFT) methods have been performed to simulate crystalline structures and infrared/Raman spectra of nylon 6.[41–43] Hofmann and his co-workers explored possible helix types with unidirectional H-bonds in the blocked octapeptide of Ahx residues at HF and B3LPY levels of theory with the 6-31G(d) basis set.[8,44] The single-point energies were also calculated using the polarizable continuum model (PCM)[45] at the HF/6-31G(d) level of theory in water. They obtained 21 helix conformers with H-bonds only in backward direction and also 21 helix conformers with the H-bonds in forward direction from the conformational search (see Figure 2 for definition of H-bonds). The H_{16}^{I} conformer was most preferred at all levels of theory both in the gas phase and water, which is a forward helix with 16-membered H-bonded pseudocycles. The next preferred helices were the conformers H_{18}^{I} and H_9^{I}, the first with all H-bonds in backward direction and the second with all H-bonds in forward direction. The H_9^{I} conformer with a flat periodic turn-like structure became a comparable stability to the other two helix types in water. ε-Amino acid residue has a unique backbone sequence resembling a dipeptide unit in α/β-hybrid peptide. The correspondence among some helices of ε-peptide and α/β-hybrid peptide was suggested as H_{11}^{X}:H_{11}^{I}, H_{11}^{II}:$H_{11/9}^{I}$, H_9^{VI}:$H_{9/11}^{I}$, H_{16}^{IV}:$H_{16/18}^{I}$, and H_{18}^{II}:$H_{18/16}^{I}$ [(helix type in ε-peptide) : (helix type in α/β-hybrid peptide)].[44]

Here, we extensively explored the conformational preferences of oligomers of ε-amino acid with a cyclopentane substitution [2-((1*R*,3*S*)-3-(aminomethyl)cyclopentyl)acetic acid, Amc$_5$a; Figure 1e] using DFT methods in chloroform and water. The preferred helical structures of the Amc$_5$a hexamer were compared with those of the canonical unsubstituted Ahx hexamer. In addition, the helical preferences were investigated for the hexamer analogue with pyrrolidines instead of cyclopentanes (Figure 1f). Chemical structure and definition of torsion angles for Amc$_5$a oligomers are defined in Figure 3.

Results and Discussion

Conformational Preferences of Amc$_5$a Oligomers

Monomer. For the Amc$_5$a monomer, we located 34 local minima with the relative free energy (ΔG_c) < 5 kcal mol^{-1} in chloroform from the conformational search and three helical structures (H_9, H_{11}, and H_{18}^{I}) of the Amc$_5$a hexamer. The corresponding backbone torsion angles, relative thermodynamic properties, and absolute electronic energies are shown in Tables S1–S3 in the Supporting Information, respectively. The backbone torsion angles and relative free energies (ΔG_c in chloroform and ΔG_w in water) of 18 local minima with $\Delta G_c < 3$ kcal mol^{-1} are listed in Table 1. The eight preferred conformers of the Amc$_5$a monomer in chloroform and water are shown in Figure 4.

In chloroform, the most preferred conformer was m-01 (populated at 31 %), which was stabilized by the C_{11} H-bond between C=O(Ac) and H–N(NHMe) with the distance 2.01 Å. The next preferred conformers are m-02, m-03, m-04, and m-05

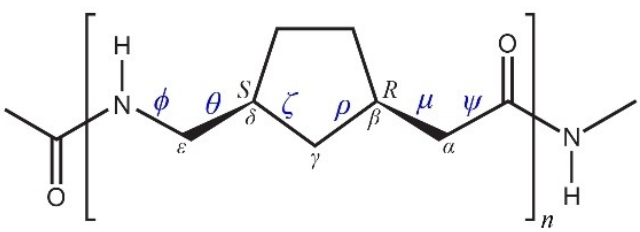

Figure 3. Chemical structure and torsion angles for Ac-(Amc$_5$a)$_n$-NHMe ($n = 1$, 2, 4, and 6). Amc$_5$a stands for 2-((1*R*,3*S*)-3-(aminomethyl)cyclopentyl)acetic acid.

Table 1. H-bond types, torsion angles (°), and relative conformational free energies (kcal mol^{-1}) of 18 local minima of the Amc$_5$a monomer calculated at the M06-2X/def2-TZVP//M06-2X/6-31 + G(d) level of theory in chloroform and water.[a]

Conformer	H-bond[b]	ϕ	θ	ζ	ρ	μ	ψ	ΔG_c[c]	ΔG_w[c]
m-01	C_{11}	104	−65	−89	113	64	−118	0.00	0.64
m-02		−78	−61	−159	167	−174	−81	0.37	0.00
m-03	C_9	105	58	−118	90	54	84	0.41	1.22
m-04		78	179	−166	163	56	85	0.50	0.30
m-05	E	78	−178	−163	166	−174	−80	0.97	0.73
m-06		103	65	−139	160	177	121	1.32	0.89
m-07		79	−174	−133	158	65	−122	1.37	0.90
m-08	(H_{16}^{I})[d]	−82	−64	−163	166	64	−133	1.65	1.28
m-09		78	−174	−135	159	178	142	1.97	1.66
m-10		−104	−180	−157	167	178	123	2.03	2.00
m-11		103	64	−138	160	64	−145	2.19	1.92
m-12		−80	−59	−143	163	176	140	2.20	1.79
m-13		109	−62	−88	114	−175	146	2.21	2.73
m-14	C_{11}	104	−70	−106	139	−90	74	2.31	2.86
m-15		−94	58	−168	165	178	144	2.32	2.23
m-16		101	63	−137	158	54	84	2.51	2.60
m-17	C_9	−81	−58	−89	118	−54	−99	2.62	3.33
m-18	C_9	101	61	−120	146	−74	−121	2.86	3.74

[a] Only conformers with $\Delta G_c < 3$ kcal mol^{-1} in chloroform. Torsion angles are defined in Figure 3. [b] C_{11} and C_9 are H-bonded structures with 11- and 9-membered pseudocycles for backbone, respectively. The extended structure was designated by "E". [c] ΔG_c and ΔG_w are relative free energies in chloroform and water, respectively. [d] H_{16}^{I} helical structure defined in Ref. [44].

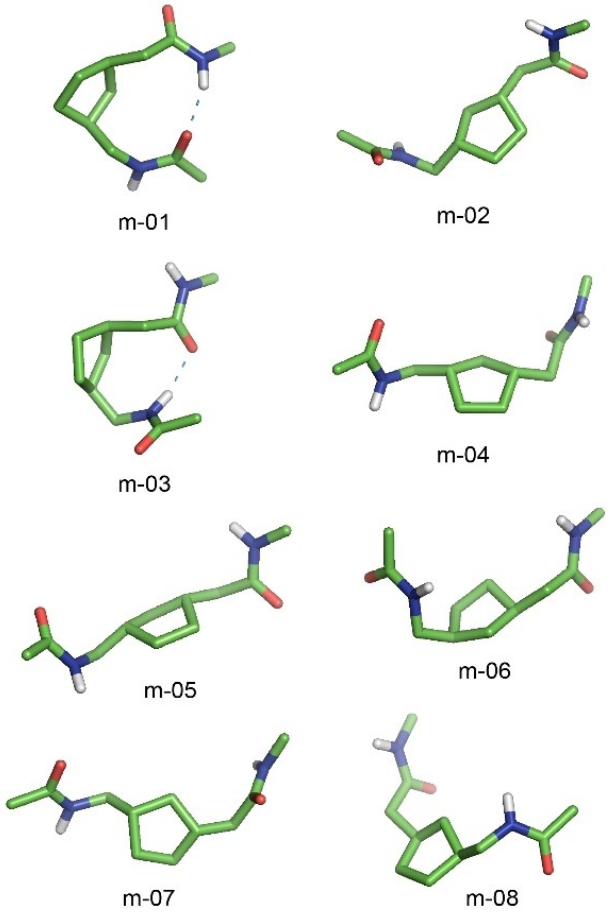

Figure 4. Preferred conformers of the Amc$_5$a monomer in chloroform and water.

with $\Delta G_c = 0.37$, 0.41, 0.50, and 0.97 kcal mol^{-1}, respectively (populated at 17, 16, 13, and 6%, respectively). In particular, conformer m-03 had a C_9 H-bond between N–H(1) and C=O(1) with the distance 2.02 Å, which probably contributed to stabilize it as the conformer with the second lowest energy ($\Delta E_c = 0.75$ kcal mol^{-1} in chloroform and $\Delta E_w = 0.92$ kcal mol^{-1} in water, Table S2 in the Supporting Information). In water, the most preferred conformer was m-02 (populated at 31%) with the absence of H-bonds and followed by conformer m-04, m-01, m-05, m-06, and m-07 with $\Delta G_w = 0.30$, 0.64, 0.73, 0.89, and 0.90 kcal mol^{-1}, respectively (populated at 19, 11, 9, 7, and 7%, respectively). Hence, there were 21 and 12% decreases of the population for H-bonded conformer m-01 and m-03, respectively, when the solvent polarity changes from chloroform to water. Although conformer m-08 is capable of forming a H_{16}^{I} helical structures for oligomers of dimer to hexamer (as discussed in Computational Details), its ΔG_c and ΔG_w values were 1.65 and 1.28 kcal mol^{-1} in chloroform and water, respectively (populated at 2 and 4%, respectively), due to the absence of the C_{16} H-bond.

Dimer. In the case of the Amc$_5$a dimer, we located 32 local minima with $\Delta G_c < 3$ kcal mol^{-1} in chloroform from the conformational search and four helical structures (H_{16}^{I}, H_9, H_{11}, and H_{18}^{I}) were also included for comparison. The corresponding backbone torsion angles, relative thermodynamic properties, and absolute electronic energies of the Amc$_5$a dimer are shown in Tables S4–S6 in the Supporting Information, respectively. The backbone torsion angles and relative free energies of 15 local minima with $\Delta G_c < 1.5$ kcal mol^{-1} are listed in Table 2. The seven preferred conformers of the Amc$_5$a dimer in chloroform and water are shown in Figure 5.

In chloroform, the most preferred conformer was the H_{16}^{I} helical structure d-01 (populated at 16%), which was stabilized by a C_{16} H-bond between N–H(1) and C=O(2) with the distance 1.93 Å. The following preferred conformers were d-02, d-03, and d-04, which had comparable values of $\Delta G_c = 0.03$, 0.03, and

Table 2. H-bond types, torsion angles (°), and relative conformational free energies (kcal mol^{-1}) of 18 local minima of the Amc$_5$a dimer calculated at the M06-2X/def2-TZVP//M06-2X/6-31 + G(d) level of theory in chloroform and water.[a]

Conformer	H-bond[b]	ϕ	θ	ζ	ρ	μ	ψ	ΔG_c[c]	ΔG_w[c]
d-01	H_{16}^{I}	−85	−70	−162	142	62	−121	0.00	0.00
		−73	−58	−164	169	63	−148		
d-02	C_{16}	103	57	−167	165	57	−116	0.03	0.55
		−75	−60	−166	166	67	117		
d-03	C_{18}	79	−173	−122	150	57	−125	0.03	0.28
		−109	63	−141	162	178	154		
d-04	C_{11}	104	−68	−88	114	65	−115	0.18	1.02
		−77	−64	−158	171	−63	−104		
d-05	C_{18}	−111	55	−168	165	64	−149	0.39	0.58
		−96	58	−164	143	174	179		
d-06	$H_{16/18}$	−95	60	−169	170	−67	88	0.77	2.20
		101	−57	−131	158	59	−142		
d-07	C_{18},C_9	135	65	−146	121	−65	−109	0.80	2.41
		−108	76	−148	168	78	−132		
d-08	C_{16}	92	−58	−164	166	70	−79	1.06	2.17
		−62	−52	−148	165	55	64		
d-09	$H_{16/18}$	−171	−67	−163	168	65	85	1.09	2.57
		100	−64	−87	108	62	−153		
d-10	C_{18}	−104	176	−167	164	−70	88	1.12	1.22
		96	63	−172	166	171	103		
d-11	C_{18}	119	−68	−167	165	57	−126	1.13	1.46
		−78	−59	−166	165	178	−92		
d-12	C_{16}	73	171	−162	148	−58	107	1.22	2.11
		87	−69	−165	159	64	−109		
d-13	$C_{16/9}$	104	60	−129	151	50	−103	1.23	1.79
		−162	60	−148	120	−64	−100		
d-14	H_{18}	−92	53	−170	158	63	−158	1.29	1.36
		−115	65	−137	160	71	−137		
d-15	C_{18},C_9	109	−59	−148	164	57	−127	1.40	3.05
		−68	−38	−94	128	−44	123		
	H_9	−82	−57	−88	118	−54	−102	3.78	5.18
		−83	−56	−89	119	−55	−99		
	H_{18}^{I}	104	−74	−109	141	−61	174	5.53	7.12
		110	−58	−129	109	−67	87		
	H_{11}	102	−69	−107	139	−90	63	7.16	8.40
		132	−60	−76	102	−152	119		

[a] Only conformers with $\Delta G_c < 1.5$ kcal mol^{-1} in chloroform. Torsion angles are defined in Figure 3. [b] C_n is the H-bond with n-membered pseudocycle for backbone. The helical structure with n-membered pseudocycle H-bonds was represented by H_n. H_{16}^{I} and H_{18}^{I} helical structures are defined in Ref. [44]. [c] ΔG_c and ΔG_w are relative free energies in chloroform and water, respectively.

0.18 kcal mol^{-1}, respectively (populated at 15, 15, and 12%, respectively) to conformer d-01. These conformers were stabilized by a C_{16} H-bond between N–H(1) and C=O(2) with the distance 1.95 Å, a C_{18} H-bond between C=O(Ac) and H–N-(NHMe) with the distance 1.98 Å, and a C_{11} H-bond between C=O(Ac) and H–N(2) with the distance 1.97 Å, respectively. The next followed conformers were d-05 with a C_{18} H-bond between C=O(Ac) and H–N(NHMe) with the distance 1.94 Å; the mixed $H_{16/18}$ helical structure d-06 with a C_{16} H-bond between N–H(1) and C=O(2) with the distance 2.09 Å; and d-07 with a C_{18} H-bond between C=O(Ac) and H–N(NHMe) with the distance 1.90 Å and a C_9 H-bond between N–H(1) and C=O(1) with the distance 2.00 Å, whose ΔG_c values were 0.39, 0.77, and 0.80 kcal mol^{-1}, respectively (populated at 8, 4, and 4%, respectively).

In water, the most preferred conformer was the H_{16}^{I} helical structure d-01 populated at 31%, which is 15% greater than that in chloroform. The following preferred conformers were d-03, d-02, and d-05 with $\Delta G_w = 0.28$, 0.55, and 0.58 kcal mol^{-1}, respectively (populated at 19, 12, and 12%, respectively). It should be noted that conformer d-07 was the lowest energy conformer both in chloroform and water, although its ΔG_c and ΔG_w values were 0.80 and 2.41 kcal mol^{-1} in chloroform and water, respectively, due to the decrease of entropic contribution (see Table S5 in the Supporting Information).

The conformational stabilities of helical structures of dimer were calculated to be in the order H_{16}^{I} (d-01, 0.00) > $H_{16/18}$ (d-06, 0.77) > $H_{16/18}$ (d-09, 1.09) > H_{18} (d-14, 1.29) > H_9 (3.78) > H_{18}^{I} (5.53) > H_{11} (7.16) in chloroform and H_{16}^{I} (d-01, 0.00) > H_{18} (d-14, 1.36) > $H_{16/18}$ (d-06, 2.20) > $H_{16/18}$ (d-09, 2.57) > H_9 (5.18) > H_{18}^{I} (7.12) > H_{11} (8.40) in water, where ΔG_c and ΔG_w values (kcal mol^{-1}) were shown in parentheses.

Tetramer. For the Amc$_5$a tetramer, we located 32 local minima with $\Delta G_c < 13$ kcal mol^{-1} in chloroform from consecutively jointing of dimers and three helical structures (H_{16}^{I}, H_9, and H_{18}^{I}), and the H_{11} helical structure was also included for comparison. The corresponding backbone torsion angles, relative thermodynamic properties, and absolute electronic energies of the Amc$_5$a tetramer are shown in Tables S7–S9 in the Supporting Information, respectively. The backbone torsion angles and relative free energies of 14 local minima with $\Delta G_c <$ 10 kcal mol^{-1} and three H_{18}^{I}, H_9 and H_{11} helical structures are

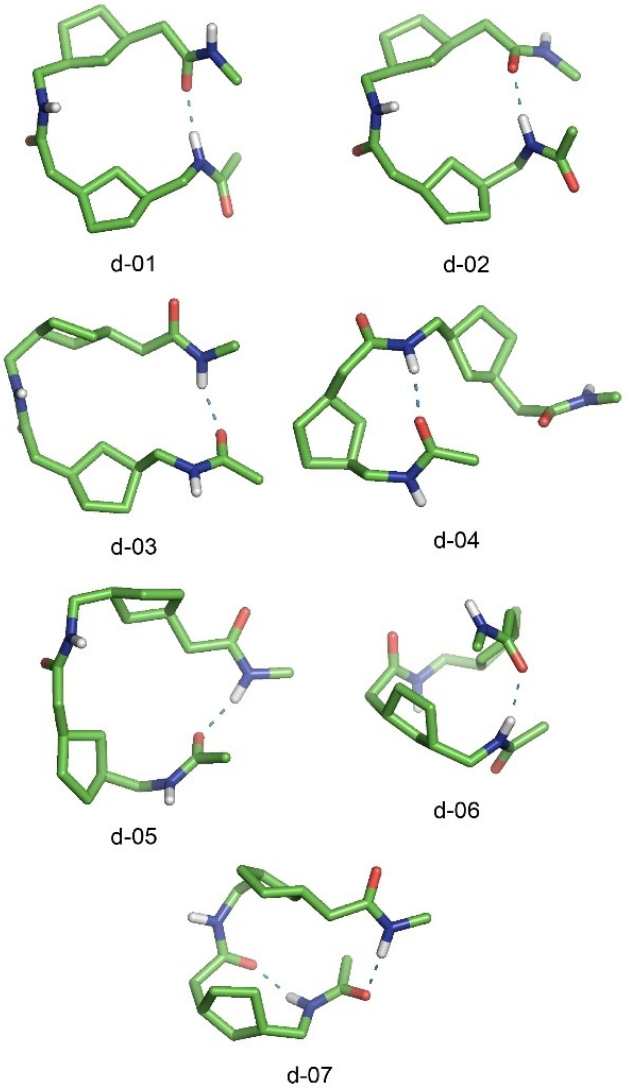

Figure 5. Preferred conformers of the Amc_5a dimer in chloroform and water.

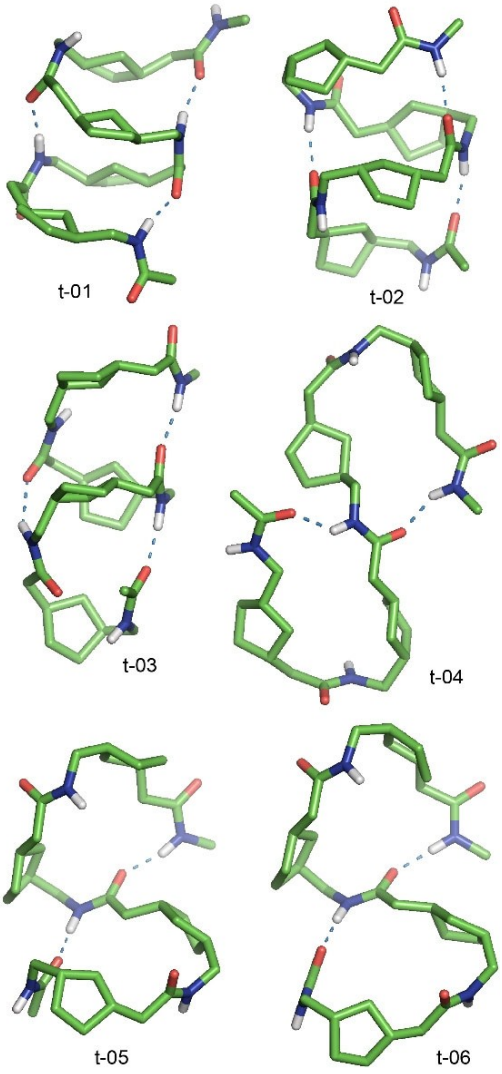

Figure 6. Preferred conformers of the Amc_5a tetramer in chloroform and water: t-01 (H_{16}^{I}), t-02 (H_{18}), t-03 ($H_{18/16}$), t-04 (2 C_{18}), t-05 (2 C_{18}), and t-06 (2 C_{18}). H-bond types in parentheses.

listed in Table 3. The six representative conformers of the Amc_5a tetramer in chloroform and water are shown in Figure 6.

Both in chloroform and water, the H_{16}^{I} helical structure t-01 was dominantly populated at 100%, which was stabilized by three C_{16} H-bonds between N–H(i) and C=O($i+1$) ($i=1$, 2, 3) with the distances 1.93–1.97 Å. The H_{18} helical structure **t**-02 with three C_{18} H-bonds between C=O($i-1$) and H–N($i+2$) ($i=1$, 2, 3) with the distances 1.94–2.03 Å was the second preferred conformer both in chloroform and water ($\Delta G_c = 5.89$ kcal mol^{-1} in chloroform and $\Delta G_w = 6.25$ kcal mol^{-1} in water).

In chloroform, the third preferred conformer was the mixed $H_{18/16}$ helical structure t-03 ($\Delta G_c = 6.21$ kcal mol^{-1}) with two C_{18} H-bonds between C=O($i-1$) and H–N($i+2$) ($i=1$, 3) with the distances 1.90 and 1.91 Å, respectively, and one C_{16} H-bond between N–H(2) and C=O(3) with the distance 2.14 Å. The fourth, fifth, and sixth preferred conformers were t-04, t-05, and t-06 with $\Delta G_c = 7.62$, 7.76, and 7.94 kcal mol^{-1}, respectively, in common stabilized by two C_{18} H-bonds between C=O($i-1$) and H–N($i+2$) ($i=1$, 3) with the distances 2.04 and 1.98 Å; 1.91 and 1.91 Å; and 1.88 and 1.86 Å, respectively. However, in water conformers t-04, t-05, and t-06 were the third, fourth, and fifth preferred conformers, respectively, stabilized by two C_{18} H-bonds with $\Delta G_w = 7.46$, 7.61, and 7.65 kcal mol^{-1}, respectively. In particular, the mixed $H_{18/16}$ helical structure t-03 became as the sixth preferred conformer with $\Delta G_w = 8.98$ kcal mol^{-1} in water.

The conformational stabilities of helical structures of tetramer were calculated to be in the order H_{16}^{I} (t-01) $\gg H_{18}$ (t-02) $> H_{18/16}$ (t-03) $> H_{16/18}$ (t-07) $> H_{18}^{I}$ (t-17) $> H_9$ (t-24) $\gg H_{11}$ both in chloroform and water with $\Delta G_c = 0.00$, 5.89, 6.21, 8.05, 10.17, 11.00, and 17.76 kcal mol^{-1} in chloroform, respectively; and $\Delta G_w = 0.00$, 6.25, 8.98, 9.65, 10.36, 12.74, and 19.40 kcal mol^{-1} in water, respectively.

Hexamer. In the case of the Amc_5a hexamer, we located 14 local minima in chloroform, of which ten local minima were obtained from preferred structures of tetramer and four helical structures were included for comparison. The corresponding backbone torsion angles and absolute electronic energies of

Table 3. H-bond types and relative thermodynamic properties (kcal mol^{-1}) of representative structures of the Amc_5a tetramers calculated at the M06-2X/def2-TZVP//M06-2X/6-31+G(d) level of theory in chloroform and water.[a]

Conformer	H-bond[b]	Chloroform ΔE_c[c]	ΔH_c[c]	ΔG_c[c]	w[d]	Water ΔE_c[c]	ΔH_c[c]	ΔG_c[c]	w[d]
t-01	H_{16}^{I}	0.00	0.00	0.00	100.0	0.00	0.00	0.00	100.0
t-02	H_{18}	2.56	3.00	5.89	0.0	2.93	3.36	6.25	0.0
t-03	$H_{18/16}$	1.64	2.31	6.21	0.0	4.41	5.08	8.98	0.0
t-04	$2C_{18}$	8.66	8.56	7.62	0.0	8.51	8.41	7.46	0.0
t-05	$2C_{18}$	9.85	9.56	7.76	0.0	9.70	9.41	7.61	0.0
t-06	$2C_{18}$	7.58	6.97	7.94	0.0	7.29	6.69	7.65	0.0
t-07	$H_{16/18}$	2.91	2.79	8.05	0.0	4.51	4.39	9.65	0.0
t-08	$2C_{18}$	9.73	10.14	8.26	0.0	9.53	9.95	8.06	0.0
t-09	$2C_{18}$,C_{30}	2.73	2.87	8.64	0.0	3.67	3.81	9.58	0.0
t-10	$2C_{18}$	10.70	10.77	8.74	0.0	10.33	10.40	8.38	0.0
t-11	$2C_{18}$	9.78	9.89	8.80	0.0	9.41	9.52	8.44	0.0
t-12	$2C_{16}$,$2C_{11}$	5.26	5.73	9.02	0.0	7.25	7.72	11.00	0.0
t-13	$2C_{11}$,C_{30}	5.43	6.13	9.58	0.0	6.30	7.00	10.45	0.0
t-14	$2C_{16/9}$	6.06	6.99	9.87	0.0	6.10	7.03	9.91	0.0
t-17	H_{18}^{I}	6.39	6.39	10.17	0.0	6.58	6.59	10.36	0.0
t-24	H_9	7.99	9.13	11.00	0.0	9.73	10.88	12.74	0.0
	H_{11}	14.58	16.05	17.76	0.0	16.21	17.69	19.40	0.0

[a] Only conformers with $\Delta G_c < 10$ kcal mol^{-1} and three helical structures in chloroform. Torsion angles are shown in Table S7 in the Supporting Information. [b] C_n is the H-bond with n-membered pseudocycle for backbone. The Helical structure with n-membered pseudocycle H-bonds was represented by H_n. H_{16}^{I} and H_{18}^{I} helical structures are defined in Ref. [44]. [c] ΔE, ΔH, and ΔG are relative electronic energy, enthalpy, and Gibbs free energy of each conformation at 25 °C and 1 atm calculated at the M06-2X/def2-TZVP//M06-2X/6-31+G(d) level of theory in chloroform and water, respectively. Each value of ΔE was calculated by the sum of $\Delta E_{0,dTZ}$ (the single-point energy at the M06-2X/def2-TZVP level of theory) and $\Delta\Delta G_{solv}$ (the solvation free energy calculated at the PCM M06-2X/6-31+G(d) level of theory). [d] Population of each conformation was calculated by its ΔG at 25 °C.

the Amc_5a hexamer are shown in Tables S10 and S11 in the Supporting Information, respectively. The H-bond types and relative thermodynamic properties of 14 local minima are listed in Table 4. The backbone torsion angles and helical parameters of seven representative helical structures are listed in Table 5 and their 3D structures are depicted in Figure 7, whose Cartesian coordinates are also listed in the Supporting Information.

In chloroform, the most preferred conformer h-01 (populated at ~100%) adopted a H_{16}^{I} helical structure with five C_{16} H-bonds between N–H(i) and C=O($i+1$) ($i=1$, 2, 3, 4, 5) with the distances 1.92–1.97 Å. The second and third preferred conformers were h-02 and h-03 with $\Delta G_c = 4.25$ and 6.58 kcal mol^{-1}, respectively. The former was a mixed $H_{18/16}$ helical structure with three C_{18} H-bonds between C=O($i-1$) and H–N($i+2$) ($i=1$, 3, 5) with the distances 1.87–1.91 Å and two C_{16} H-bonds between N–H(i) and C=O($i+1$) ($i=2$, 4) with the distances 2.21 and 2.09 Å. The latter was a H_{18} helical structure stabilized by five C_{18} H-bonds between C=O($i-1$) and H–N($i+2$) ($i=1$, 2, 3, 4, 5) with the distances 1.93–2.08 Å. The fourth preferred con-

Table 4. H-bond types and relative thermodynamic properties (kcal mol^{-1}) of representative structures of the Amc_5a hexamers calculated at the M06-2X/def2-TZVP//M06-2X/6-31+G(d) level of theory in chloroform and water.[a]

Conformer	H-bond[b]	Chloroform ΔE_c[c]	ΔH_c[c]	ΔG_c[c]	w[d]	Water ΔE_c[c]	ΔH_c[c]	ΔG_c[c]	w[d]
h-01	H_{16}^{I}	0.00	0.00	0.00	99.9	0.00	0.00	0.00	100.0
h-02	$H_{18/16}$	1.95	2.57	4.25	0.1	4.89	5.50	7.18	0.0
h-03	H_{18}	4.62	5.02	6.58	0.0	4.95	5.34	6.91	0.0
h-04	$H_{16/18}$	3.94	4.85	8.87	0.0	6.80	7.71	11.73	0.0
h-05	$H_{16/18}$	7.03	7.95	10.22	0.0	9.29	10.21	12.48	0.0
h-06	$3C_{18}$	14.46	14.37	10.82	0.0	13.44	13.35	9.80	0.0
h-07	$H_{18/16}$	7.43	8.38	12.81	0.0	10.35	11.30	15.73	0.0
h-08	$3C_{11/18}$	14.24	15.83	15.68	0.0	13.97	15.56	15.41	0.0
h-09	$2C_{16}$,$2C_{11}$	12.14	12.25	16.04	0.0	13.99	14.10	17.88	0.0
h-10	$3C_{16/9}$	13.49	14.77	16.77	0.0	12.80	14.09	16.09	0.0
h-11	H_{18}^{I}	14.79	15.36	16.99	0.0	15.24	15.81	17.44	0.0
h-12	$3C_{16}$	16.78	17.39	18.40	0.0	17.87	18.48	19.49	0.0
h-13	H_9	16.16	18.12	18.78	0.0	17.95	19.92	20.57	0.0
h-14	H_{11}	26.31	27.89	29.42	0.0	28.03	29.61	31.14	0.0

[a] Torsion angles are shown in Table S10 in the Supporting Information. [b] C_n is the H-bond with n-membered pseudocycle for backbone. The Helical structure with n-membered pseudocycle H-bonds was represented by H_n. H_{16}^{I} and H_{18}^{I} helical structures are defined in Ref. [44]. [c] ΔE, ΔH, and ΔG are relative electronic energy, enthalpy, and Gibbs free energy of each conformation at 25 °C and 1 atm calculated at the M06-2X/def2-TZVP//M06-2X/6-31+G(d) level of theory in chloroform and water, respectively. Each value of ΔE was calculated by the sum of $\Delta E_{0,dTZ}$ (the single-point energy at the M06-2X/def2-TZVP level of theory) and $\Delta\Delta G_{solv}$ (the solvation free energy calculated at the PCM M06-2X/6-31+G(d) level of theory). [d] Population of each conformation was calculated by its ΔG at 25 °C.

Table 5. Torsion angles (°) and helical parameters of representative helical structures of the Amc_5a hexamer optimized at the M06-2X/6-31+G(d) level of theory.[a]

Conformer	H-bond[b]	ϕ	θ	ζ	ρ	μ	ψ	Helix type[c]	m[d]	p[e]
h-01	H_{16}^{I}	−78	−63	−166	166	54	−106	(*M*)-2.3_{16}	2.3	4.8
		−80	−66	−154	164	58	−126			
		−71	−58	−161	168	52	−127			
		−74	−54	−167	164	58	−122			
		−72	−57	−166	155	60	−111			
		−76	−61	−146	162	65	122			
h-02	$H_{18/16}$	−114	56	−129	155	−61	125	(*P*)-$3.5_{18/16}$	3.5	8.9
		158	−62	−136	157	64	−102			
		−95	63	−168	168	−52	108			
		173	−63	−130	155	65	−110			
		−99	64	−159	172	−55	98			
		179	−60	−133	158	62	−109			
h-03	H_{18}	−94	48	−162	136	62	−139	(*P*)-2.4_{18}	2.4	5.6
		−99	48	−174	161	61	−130			
		−106	52	−171	159	69	−143			
		−101	51	−157	165	71	−151			
		−106	56	−132	154	73	−164			
		−105	56	−114	135	65	−178			
h-04	$H_{16/18}$	−156	−70	−166	162	59	85	(*M*)-$2.2_{16/18}$	2.2	4.9
		105	−65	−96	121	61	164			
		−60	−48	−167	147	53	22			
		118	−60	−157	164	48	−132			
		−81	−63	−173	161	54	76			
		115	−61	−84	102	64	−153			
h-11	H_{18}^{I}	176	−62	−129	158	−53	108	(*M*)-3.8_{18}	3.8	8.4
		111	−67	−143	168	−52	114			
		123	−65	−157	170	−61	87			
		169	−60	−156	138	−55	105			
		142	−73	−123	153	−61	171			
		105	−72	−102	134	−61	132			
h-13	H_9	−80	−57	−88	118	−54	−101	(*P*)-2.8_9	2.8	10.9
		−84	−55	−89	119	−55	−102			
		−83	−55	−88	118	−55	−101			
		−83	−54	−89	118	−55	−101			
		−84	−54	−89	119	−56	−102			
		−82	−55	−90	119	−55	−101			
h-14	H_{11}	103	−68	−107	139	−89	63	(*P*)-3.1_{11}	3.1	11.9
		130	−58	−77	104	−153	119			
		102	−69	−107	139	−88	62			
		129	−60	−77	105	−149	117			
		100	−70	−106	139	−88	62			
		131	−60	−77	103	−152	118			

[a] Torsion angles are defined in Figure 3. [b] The helical structure with *n*-membered pseudocycle H-bonds was represented by H_n. H_{16}^{I} and H_{18}^{I} helical structures are defined in Ref. [44]. [c] (*M*) and (*P*) stand for left- and right-handed helices, respectively. [d] Number of residues per turn. [e] Rise per turn (pitch) (Å).

former h-04 ($\Delta G_c = 8.87$ kcal mol^{-1}) was a mixed $H_{16/18}$ helical structure with three C_{16} H-bonds between N–H(*i*) and C=O($i+1$) ($i = 1, 3, 5$) with the distances 1.90–2.02 Å and two C_{18} H-bonds between C=O($i-1$) and H–N($i+2$) ($i = 2, 4$) with the distances 1.98 and 1.94 Å.

In water, the most preferred conformer h-01 (populated at ~100%) adopted a H_{16}^{I} helical structure as in chloroform. However, the second and third preferred conformers were the H_{18} helical structure h-03 and the mixed $H_{18/16}$ helical structure h-02 with $\Delta G_w = 6.91$ and 7.18 kcal mol^{-1}, respectively. In particular, the fourth preferred conformer h-06 ($\Delta G_w = 9.80$ kcal mol^{-1}) adopted a folded structure with three C_{18} H-bonds between C=O($i-1$) and H–N($i+2$) ($i = 1, 3, 5$) with the distances 1.86–1.89 Å as similar to the tetramer t-06, which was the sixth preferred conformer ($\Delta G_c = 10.82$ kcal mol^{-1}) in chloroform. The fifth preferred conformer was the mixed $H_{16/18}$ helical structure h-04 with $\Delta G_w = 11.73$ kcal mol^{-1} in water.

Helical structures H_{18}^{I} (h-11), H_9 (h-13), and H_{11} (h-14) had favorable four C_{18} H-bonds with the distances 1.95–2.03 Å; six C_9 H-bonds between N–H and C=O of every residue with the distances 1.98–2.03 Å; and six C_{11} H-bonds between C=O($i-1$) and H–N($i+1$) of every residue *i* with the distances 1.94–2.02 Å, respectively. However, relative free energies of these three helical structures were greater than 17 kcal mol^{-1} both in chloroform and water.

Hence, the conformational stabilities of helical structures of hexamer were calculated to be in the order $H_{16}^{I} \gg H_{18/16} > H_{18} > H_{16/18} \gg H_{18}^{I} > H_9 \gg H_{11}$ in chloroform and $H_{16}^{I} \gg H_{18} > H_{18/16} > H_{16/18} \gg H_{18}^{I} > H_9 \gg H_{11}$ in water. The helical parameters of seven representative helical structures of the Amc_5a hexamer are shown in Table 5. The helical types of H_{16}^{I} (h-01), $H_{16/18}$ (h-04),

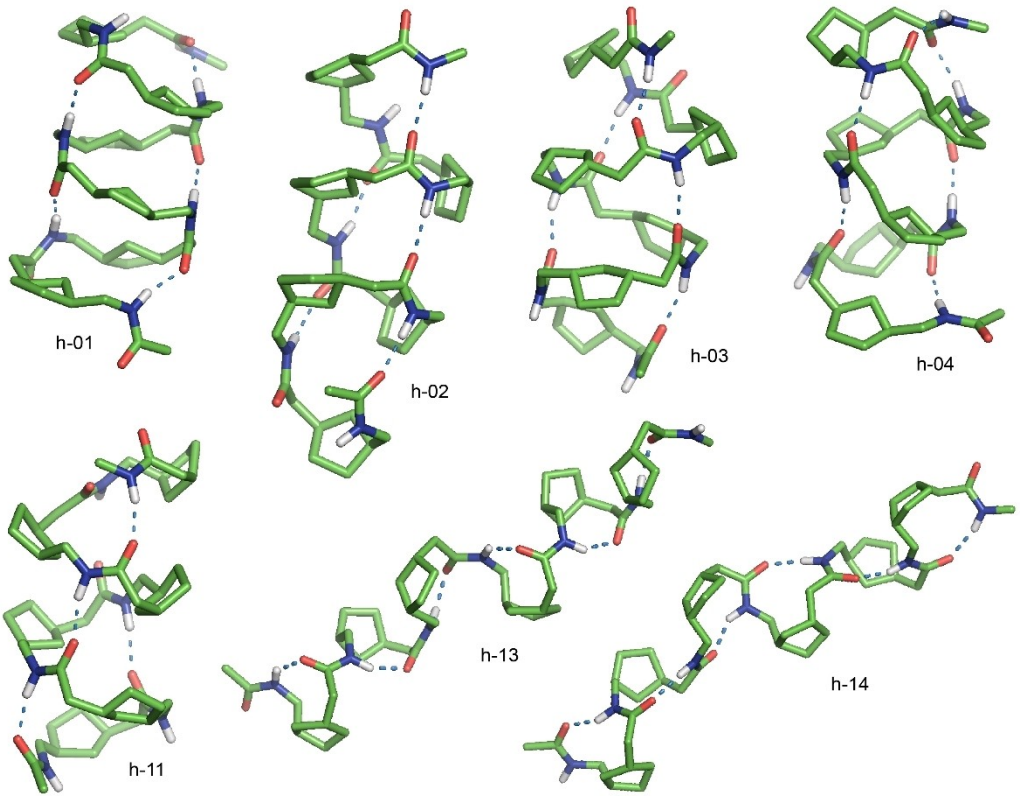

Figure 7. Preferred helical conformers of the Amc_5a hexamer in chloroform and water: h-01 (H_{16}^{I}), h-02 ($H_{18/16}$), h-03 (H_{18}), h-04 ($H_{16/18}$), h-11 (H_{18}^{I}), h-13 (H_9), and h-14 (H_{11}). H-bond types in parentheses.

and H_{18}^{I} (h-11) structures are left-handed (*M*)-2.3_{16} with a rise of 4.8 Å per turn, (*M*)-$2.2_{16/18}$ with a rise of 4.9 Å per turn, and (*M*)-3.8_{18} with a rise of 8.4 Å per turn, respectively. However, the helical types of $H_{18/16}$ (h-02), H_{18} (h-03), H_9 (h-13), and H_{11} (h-14) structures are right-handed (*P*)-$3.5_{18/16}$ with a rise of 8.9 Å per turn, (*P*)-2.4_{18} with a rise of 5.6 Å per turn, (*P*)-2.8_9 with a rise of 10.9 Å per turn, and (*P*)-3.1_{11} with a rise of 11.9 Å per turn, respectively.

Helical Preferences of Ahx and Ampa Hexamers

Next, we compared the helical preferences of Ahx and Ampa hexamers to investigate the changes in helical preference of ε-peptides by introducing cyclopentanes and pyrrolidines into the backbone of the sequence. For the unsubstituted Ahx hexamer (see Figure 1a), we optimized nine helical structures (H_{18}^{I}, H_{16}^{I}, H_{18}, $H_{16/18}$, $H_{18/16}$, H_9^{I}, H_{11}^{I}, and H_{11}) at the M06-2X/6-31+G(d) level of theory, of which four types of H_{18}^{I}, H_{16}^{I}, H_9^{I}, and H_{11}^{I} were considered in Ref. [44]. The backbone torsion angles and absolute electronic energies of the Ahx hexamer are shown in Tables S12 and S13 in the Supporting Information, respectively. The H-bond types and relative thermodynamic properties of nine helical structures are listed in Table 6. The structures of three most preferred conformers in chloroform and water are depicted in Figure 8, whose Cartesian coordinates are also listed in the Supporting Information.

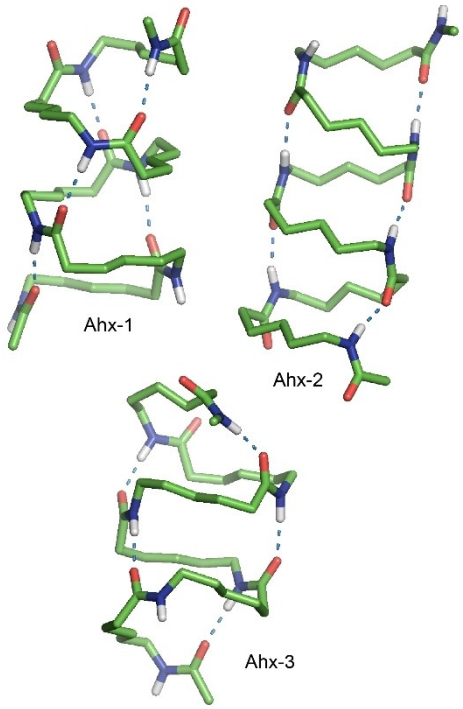

Figure 8. Preferred helical conformers of the Ahx hexamer in chloroform and water: Ahx-1 (H_{18}^{I}), Ahx-2 (H_{16}^{I}), and Ahx-3 (H_{18}). H-bond types in parentheses.

Table 6. H-bond types and relative thermodynamic properties (kcal mol^{-1}) of helical structures of the Ahx hexamers calculated at the M06-2X/def2-TZVP//M06-2X/6-31+G(d) level of theory in chloroform and water.[a]

Conformer	H-bond[b]	Chloroform				Water			
		ΔE_c[c]	ΔH_c[c]	ΔG_c[c]	w[d]	ΔE_c[c]	ΔH_c[c]	ΔG_c[c]	w[d]
Ahx-1	H_{18}^{I}	0.00	0.00	0.00	96.5	0.00	0.00	0.00	91.4
Ahx-2	H_{16}^{I}	6.10	6.84	2.18	2.4	5.36	6.09	1.43	8.1
Ahx-3	H_{18}	2.51	2.63	2.70	1.0	2.92	3.04	3.11	0.5
Ahx-4	$H_{16/18}$	7.98	8.71	9.58	0.0	10.15	10.87	11.75	0.0
Ahx-5	$H_{18/16}$	8.82	10.01	10.27	0.0	11.58	12.77	13.03	0.0
Ahx-6	$H_{16/18}$	10.22	11.22	11.78	0.0	12.77	13.77	14.34	0.0
Ahx-7	H_{9}^{I}	18.65	20.45	12.09	0.0	20.58	22.39	14.02	0.0
Ahx-8	H_{11}^{I}	23.69	25.86	17.60	0.0	25.43	27.59	19.34	0.0
Ahx-9	H_{11}	25.71	27.56	23.16	0.0	27.99	29.84	25.44	0.0

[a] Torsion angles are shown in Table S13 in the Supporting Information. [b] The helical structure with *n*-membered pseudocycle H-bonds was represented by H_n. H_{18}^{I}, H_{16}^{I}, H_9^{I}, and H_{11}^{I} helical structures are defined in Ref. [44]. [c] ΔE, ΔH, and ΔG are relative electronic energy, enthalpy, and Gibbs free energy of each conformation at 25 °C and 1 atm calculated at the M06-2X/def2-TZVP//M06-2X/6-31+G(d) level of theory in chloroform and water, respectively. Each value of ΔE was calculated by the sum of $\Delta E_{0,dTZ}$ (the single-point energy at the M06-2X/def2-TZVP level of theory) and $\Delta\Delta G_{solv}$ (the solvation free energy calculated at the PCM M06-2X/6-31+G(d) level of theory). [d] Population of each conformation was calculated by its ΔG at 25 °C.

Both in chloroform and water, the most preferred conformer Ahx-1 adopted a left-handed (*M*)-2.4$_{18}$ type of the H_{18}^{I} helical structure with a rise of 4.6 Å per turn (populated at 97% in chloroform and 91% in water) stabilized by five C_{18} H-bonds between C=O(i−1) and H–N(i+2) (i=1, 2, 3, 4, 5) with the distances 1.88–1.94 Å. The second and third preferred conformers Ahx-2 and Ahx-3 were the H_{16}^{I} and H_{18} helical structures with ΔG_c=2.18 and 2.70 kcal mol^{-1} in chloroform and ΔG_w= 1.43 and 3.11 kcal mol^{-1} in water, respectively. The former Ahx-2 structure were stabilized by five C_{16} H-bonds between N–H(i) and C=O(i+1) (i=1, 2, 3, 4, 5) with the distances 1.88–1.92 Å, whereas the latter Ahx-3 was stabilized by five C_{18} H-bonds between C=O(i−1) and H–N(i+2) (i=1, 2, 3, 4, 5) with the distances 1.88–1.94 Å.

The conformational stabilities of helical structures of the Ahx hexamer were calculated to be in the order $H_{18}^{I} > H_{16}^{I} > H_{18} \gg H_{16/18} > H_{18/16} > H_9^{I} \gg H_{11}^{I} \gg H_{11}$ both in chloroform and water. However, Schramm and Hofmann estimated the helical propensity of the Ahx hexamer in the order H_{16}^{I} (0.0) > H_{18}^{I} (1.0) ≫ H_9^{I} (5.6) ≫ H_{11}^{I} (44.8) at the PCM HF/6-31G(d) level of theory in water, where relative energies (kcal mol^{-1}) are shown in parentheses and also confirmed the H_{16}^{I} helical structures as the lowest-energy conformer at HF/6-31G(d) and B3LYP/6-31G(d) levels of theory in the gas phase.[44]

In addition, we designed an analogue Ampa (Figure 1f) hexamer from the Amc$_5$a hexamer by incorporating pyrrolidines instead of cyclopentanes into the backbone of the sequence. The eight helical structures of the Ampa hexamer were optimized at the M06-2X/6-31+G(d) level of theory. The backbone torsion angles and absolute electronic energies of the Ampa hexamer are shown in Tables S14 and S15 in the Supporting Information, respectively. The H-bond types and relative thermodynamic properties of nine helical structures are listed in Table 7. The structures of three most preferred conformers in chloroform and water are depicted in Figure 9, whose Cartesian coordinates are listed in the Supporting Information.

In chloroform, the most preferred conformer Ampa-1 adopted a right-handed (*P*)-2.9$_{18/16}$ type of the mixed $H_{18/16}$ helical structure with a rise of 5.5 Å per turn (populated at 98%), which was stabilized by three C_{18} H-bonds between C=O(i−1) and H–N(i+2) (i=1, 3, 5) with the distances 1.90–2.04 Å and two C_{16} H-bonds between N–H(i) and C=O(i+1) (i= 2, 4) with the distances 1.96 and 1.93 Å. In particular, there were

Table 7. H-bond types and relative thermodynamic properties (kcal mol^{-1}) of helical structures of the Ampa hexamers calculated at the M06-2X/def2-TZVP//M06-2X/6-31+G(d) level of theory in chloroform and water.[a]

Conformer	H-bond[b]	Chloroform				Water			
		ΔE_c[c]	ΔH_c[c]	ΔG_c[c]	w[d]	ΔE_c[c]	ΔH_c[c]	ΔG_c[c]	w[d]
Ampa-1	$H_{18/16}$	0.00	0.00	0.00	98.1	0.00	0.12	0.23	34.2
Ampa-2	$H_{16/18}$	2.78	1.78	2.39	1.7	0.87	0.00	0.71	15.1
Ampa-3	H_{16}^{I}	7.53	6.53	3.92	0.1	3.39	2.52	0.00	50.0
Ampa-4	H_9	12.32	12.25	6.23	0.0	10.75	10.80	4.88	0.0
Ampa-5	$H_{16/18}$	6.17	6.29	7.06	0.0	5.76	6.01	6.87	0.0
Ampa-6	H_{18}	8.86	7.63	7.25	0.0	3.85	2.74	2.46	0.8
Ampa-7	H_{18}^{I}	9.21	9.54	10.95	0.0	9.38	9.83	11.35	0.0
Ampa-8	H_{11}	16.34	16.55	11.83	0.0	15.76	16.09	11.47	0.0

[a] Torsion angles are shown in Table S15 in the Supporting Information. [b] The helical structure with *n*-membered pseudocycle H-bonds was represented by H_n. H_{16}^{I} and H_{18}^{I} helical structures are defined in Ref. [44]. [c] ΔE, ΔH, and ΔG are relative electronic energy, enthalpy, and Gibbs free energy of each conformation at 25 °C and 1 atm calculated at the M06-2X/def2-TZVP//M06-2X/6-31+G(d) level of theory in chloroform and water, respectively. Each value of ΔE was calculated by the sum of $\Delta E_{0,dTZ}$ (the single-point energy at the M06-2X/def2-TZVP level of theory) and $\Delta\Delta G_{solv}$ (the solvation free energy calculated at the PCM M06-2X/6-31+G(d) level of theory). [d] Population of each conformation was calculated by its ΔG at 25 °C.

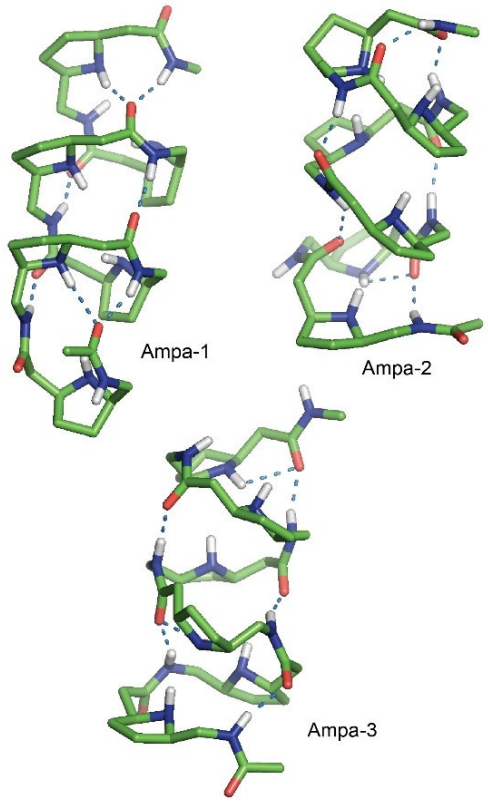

Figure 9. Preferred helical conformers of the Ampa hexamer in chloroform and water: Ampa-1 ($H_{18/16}$), Ampa-2 ($H_{16/18}$), and Ampa-3 (H_{16}^{I}). H-bond types in parentheses.

two additional C_{14} H-bonds for conformer Ampa-1 between C=O($i-1$) and H–N($i+2$) of pyrrolidine ($i=1$, 5) with the distances 2.27 and 2.06 Å. The second and third preferred conformers were Ampa-2 and Ampa-3, which are the mixed $H_{16/18}$ helical structure and the H_{16}^{I} helical structure with $\Delta G_c = 2.39$ and 3.92 kcal mol^{-1} in chloroform, respectively. The former Ampa-2 structure were stabilized by three C_{16} H-bonds between N–H(i) and C=O($i+1$) ($i=1$, 3, 5) with the distances 1.90–2.00 Å and two C_{18} H-bonds between C=O($i-1$) and H–N($i+2$) ($i=2$, 4) with the distances 2.19 and 1.90 Å. The latter Ampa-3 structure had five C_{16} H-bonds between N–H(i) and C=O($i+1$) ($i=1$, 2, 3, 4, 5) with the distances 1.93–2.08 Å. However, a left-handed (M)-2.4$_{16}$ type of the H_{16}^{I} helical structure (Ampa-3) with a rise of 4.7 Å per turn was dominantly populated at 50% in water and coexisted with the mixed $H_{18/16}$ and $H_{16/18}$ helical structures (Ampa-1 and Ampa-2, respectively) with $\Delta G_w = 0.23$ and 0.71 kcal mol^{-1}, respectively (populated at 34 and 15%, respectively).

The conformational stabilities of helical structures of the Ampa hexamer were calculated to be in the order $H_{18/16} \gg H_{16/18} > H_{16}^{I} \gg H_9 > H_{18} \gg H_{18}^{I} > H_{11}$ in chloroform and $H_{16}^{I} > H_{18/16} > H_{16/18} > H_{18} \gg H_9 \gg H_{18}^{I} \approx H_{11}$ in water (see the values of ΔG_c and ΔG_w in Table 7). These helical propensities of the Ampa hexamer are quite different from those of Amc$_5$a and Ahx hexamers, as described above. Hence, hexamers of ε-amino acid residues exhibited different preferences of helical structures depending on the substituents in peptide backbone and the solvent polarity as well as the chain length. In particular, the strong preference of the left-handed H_{16}^{I} helical structure for the Amc$_5$a hexamer with cyclopentane substituents in chloroform and water and the right-handed mixed $H_{18/16}$ and left-handed H_{16}^{I} helical structures for the Ampa hexamer with pyrrolidine substituents in chloroform and water, respectively, may suggest us the possibility of their use in designing bioactive helical peptides in nonpolar or polar solvents.

Conclusion

The conformational preferences of oligopeptides of an ε-amino acid (Amc$_5$a) with a cyclopentane substituent in the C^{β}–C^{γ}–C^{δ} sequence of the peptide backbone were investigated using DFT methods in chloroform and water. The H_{16} helical structure was the most preferred conformation of the Amc$_5$a oligomers (dimer to hexamer) both in chloroform and water, although the H_{16} helical structure and folded structures with C_n H-bonded pseudocycles coexisted for the Amc$_5$a dimer. Four residues were found to be sufficient to induce a substantial H_{16} helix population in solution.

The Amc$_5$a hexamer adopted a stable left-handed (M)-2.3$_{16}$ helical conformation with a rise of 4.8 Å per turn, whereas the hexamer of the unsubstituted Ahx residue dominantly exhibited a (M)-2.4$_{18}$ helical conformation. The hexamer of Ampa (an analogue of Amc$_5$a with cyclopentane replaced by pyrrolidine) adopted the right-handed mixed (P)-2.9$_{18/16}$ helical conformation in chloroform and the (M)-2.4$_{16}$ helical conformation in water. The solvation free energy was found to be crucial to stabilize the left-handed (M)-2.3$_{16}$ helical conformation for the Amc$_5$a hexamer both in chloroform and water.

Hence, hexamers of ε-amino acid residues exhibited different preferences of helical structures depending on the substituent in peptide backbone and the solvent polarity as well as the chain length. In particular, the strong propensity to form specific types of helical structures for the Amc$_5$a/Ampa hexamer with cyclopentane/pyrrolidine substituents in solution may suggest the possibility of their use in designing bioactive helical peptides in nonpolar or polar solvents.

Computational Methods

Chemical structure and definition of torsion angles for Amc$_5$a oligomers are defined in Figure 3. GaussView[46] was used for the generation of initial structures and the peptide structure editing. All HF and DFT calculations were carried out using the Gaussian 09 programs.[47] All DFT calculations were performed using the M06-2X functional method.[48] The M06-2X is a hybrid-meta-GGA functional with an improved medium-range correlation energy. For all local minima of Amc$_5$a oligomers optimized at the M06-2X/6-31+G(d) level of theory, the relative energies (ΔE_s) of each local minimum in chloroform and water were calculated as the sum of the relative single-point energy ($\Delta E_{0,dTZ}$) at the M06-2X/def2-TZVP level of theory and the relative solvation free energies ($\Delta\Delta G_{solv}$) obtained at the M06-2X/6-31+G(d) level of theory using the PCM[45] method. Vibrational frequencies were calculated for all local minima at the

M06-2X/6-31+G(d) level of theory at 25 °C and 1 atm. The scale factor used is 0.9440 that was chosen to reproduce experimental frequency of 1707 cm^{-1} for the amide I band of *N*-methylacetamide in Ar and N_2 matrixes.[49] The zero-point energy correction and the thermal energy corrections were employed in calculating the Gibbs free energy of each conformation, from which enthalpic and entropic contributions (i.e., $\Delta\Delta H$ and $-T\Delta\Delta S$, respectively) were computed. The relative Gibbs free energy (ΔG_s) of each local minimum in solution was calculated by the sum of ΔE_s, $\Delta\Delta H$, and $-T\Delta\Delta S$, from which the populations of all local minima were estimated at 25 °C in solution. Here, the ideal gas, rigid rotor, and harmonic oscillator approximations were used for the translational, rotational, and vibrational contributions to the Gibbs free energy, respectively.[50] Recently, the M06-2X/def2-TZVP//M06-2X/6-31+G(d) level of theory with the PCM method appeared to be appropriate in predicting the conformational preferences and the *cis–trans* isomerization of the longer peptides containing Pro or Pro derivatives in chloroform.[51]

First, we performed the conformational search of monomer and dimer of Amc_5a residues in order to investigate the feasible initial structures of short Amc_5a peptides. The 648 and 949 initial structures were generated for monomer and dimer of Amc_5a residues, respectively, by the systematic search of the Discovery Studio package[52] using the CHARMm force field with the maximum systematic conformations = 1000 and the energy threshold = 20 kcal mol^{-1}. In the conformational search, a systematic variation of each of the torsion angles Φ, θ, μ, and ψ of the backbone (Figure 3) was done using steps of 60°. These initial structures were optimized at the HF/3-21G(d) level of theory and we obtained 63 and 168 local minima for monomer and dimer of Amc_5a residues, respectively, with the relative energy (ΔE_0) < 10 kcal mol^{-1}, which were reoptimized at M06-2X/6-31G(d) and M06-2X/6-31+G(d) levels of theory. Hence, we located 41 monomer and 91 dimer structures with ΔE_0 < 10 kcal mol^{-1} at the M06-2X/6-31+G(d) level of theory. For the tetramer, the initial structures were built by consecutively jointing of 62 dimers with ΔE_0 < 6 kcal mol^{-1} at the M06-2X/6-31+G(d) level of theory and reoptimized at M06-2X/6-31G(d) and M06-2X/6-31+G(d) levels of theory. Finally, we obtained 44 local minima of tetramer at the M06-2X/6-31+G(d) level of theory. Then, 13 local minima of tetramer with the relative Gibbs free energy (ΔG_c) < 4 kcal mol^{-1} in chloroform were used to generate the initial structures of the hexamer and reoptimized at M06-2X/6-31G(d) and M06-2X/6-31+G(d) levels of theory.

Feasible H-bond types in Amc_5a oligomers are depicted in Figure 2; C_n denotes the H-bonded pseudocyle with *n* atoms (C_9, C_{16}, and C_{23} H-bonds in forward direction; C_{11}, C_{18}, and C_{25} H-bonds in backward direction). In this work, only helical structures with C_9, C_{16}, C_{11}, and C_{18} H-bonds were considered for Amc_5a oligomers due to the very high relative energies of C_{23} and C_{25} H-bonded helical conformations for the Ahx octamer.[44] Torsion angles of helical structures of the Ahx octamer with C_9, C_{16}, C_{11}, and C_{18} H-bonds[44] were used to generate initial helical structures for the Amc_5a hexamer. We obtained only six helical structures (H_9^{III}, H_9^{IV}, H_{16}^{II}, H_{11}^{VII}, H_{18}^{I}, and H_{18}^{IV} types) for the Amc_5a hexamer, which were optimized at the M06-2X/6-31G(d) level of theory. However, three H_9^{IV}, H_{16}^{II}, and H_{18}^{IV} helical structures of the Amc_5a hexamer exhibited higher conformational energies than H_9^{III}, H_{16}^{I}, and H_{18}^{I} helical structures, respectively. Hence, only three helical structures (H_9^{III}, H_{11}^{VII}, and H_{18}^{I} types) of the Amc_5a hexamer were optimized at the M06-2X/6-31+G(d) level of theory. Because the optimized backbone torsion angles of H_9^{III} and H_{11}^{VII} helical structures of the Amc_5a hexamer were somewhat different from those of the Ahx octamer, they were represented as H_9 and H_{11} in this work, respectively. Although the H_{16}^{I} helical structure of the Ahx octamer was found as the most stable one at all three HF/6-31G(d), B3LYP/6-31G(d), and PCM HF/6-31G(d) levels of theory, its torsion angles were not correctly reported in Ref. [44]. Hence, the initial H_{16}^{I} helical structure of the Amc_5a hexamer was built by using conformer m-08 of the Amc_5a monomer (Table 1) and the structure depicted in Figure 2 of Ref. [44] and optimized at the M06-2X/6-31+G(d) level of theory. From H_9, H_{11}, H_{16}^{I}, and H_{18}^{I} helical structures of the Amc_5a hexamer optimized at the M06-2X/6-31+G(d) level of theory, the corresponding helical structures of monomer, dimer, and tetramer were generated and optimized at the same level of theory. The helical parameters of hexamers were calculated from a set of six consecutive δ-carbons (see Figure 3) with the HELFIT program,[53] which uses the total least squares algorithm for helix fitting and requires at least four data points for the analysis. All 3D graphics of optimized structures of oligomers were prepared using PyMOL.[54]

Acknowledgements

This research was supported by the Basic Science Research Program through the National Research Foundation of Korea (NRF) funded by the Ministry of Education (2020R1I1A3053400).

Conflict of Interest

The authors declare no conflict of interest.

Data Availability Statement

The data that support the findings of this study are available in the supplementary material of this article.

Keywords: conformational analysis · DFT calculations · ε-peptides · helical foldamers · solvation effects

[1] S. H. Gellman, *Acc. Chem. Res.* **1998**, *31*, 173–180.
[2] D. J. Hill, M. J. Mio, R. B. Prince, T. S. Hughes, J. S. Moore, *Chem. Rev.* **2001**, *101*, 3893–4011.
[3] D. Seebach, A. K. Beck, D. J. Bierbaum, *Chem. Biodivers.* **2004**, *1*, 1111–1239.
[4] *Foldamers: Structure, Properties and Applications* (Eds.: S. Hecht, I. Huc), Wiley-VCH, Weinheim **2007**.
[5] I. Saraogi, A. D. Hamilton, *Chem. Soc. Rev.* **2009**, *38*, 1726–1743.
[6] P. G. Vasudev, S. Chatterjee, N. Shamala, P. Balaram, *Chem. Rev.* **2011**, *111*, 657–687.
[7] T. A. Martinek, F. Fülöp, *Chem. Soc. Rev.* **2012**, *41*, 687–702.
[8] C. Baldauf, H.-J. Hofmann, *Helv. Chim. Acta* **2012**, *95*, 2348–2383.
[9] E. A. John, C. J. Massena, O. B. Berryman, *Chem. Rev.* **2020**, *120*, 2759–2782.
[10] C. Baldauf, R. Günther, H.-J. Hofmann, *Helv. Chim. Acta* **2003**, *86*, 2573–2588.
[11] C. Baldauf, R. Günther, H.-J. Hofmann, *J. Org. Chem.* **2004**, *69*, 6214–6220.
[12] C. Baldauf, R. Günther, H.-J. Hofmann, *Angew. Chem. Int. Ed.* **2004**, *43*, 1594–1597; *Angew. Chem.* **2004**, *116*, 1621–1624.
[13] C. Baldauf, R. Günther, H.-J. Hofmann, *J. Org. Chem.* **2005**, *70*, 5351–5361.
[14] C. Baldauf, R. Günther, H.-J. Hofmann, *J. Org. Chem.* **2006**, *71*, 1200–1208.
[15] L. Mathieu, B. Legrand, C. Deng, L. Vezenkov, E. Wenger, C. Didierjean, M. Amblard, M. C. Averlant-Petit, N. Masurier, V. Lisowski, J. Martinez, L. T. Maillard, *Angew. Chem. Int. Ed.* **2013**, *52*, 6006–6010; *Angew. Chem.* **2013**, *125*, 6122–6126.

[16] B. J. Byun, Y. K. Kang, *Biopolymers* **2014**, *101*, 87–95.
[17] J. Y. Lee, C. H. Chae, Y. K. Kang, *New J. Chem.* **2014**, *38*, 966–973.
[18] Y. K. Kang, J. Y. Lee, *New J. Chem.* **2015**, *39*, 3241–3249.
[19] Y. K. Kang, H. S. Park, *Heliyon* **2020**, *6*, e04721.
[20] H. S. Park, Y. K. Kang, *ChemPlusChem* **2021**, *86*, 533–539.
[21] G. N. Tew, R. W. Scott, M. L. Klein, W. F. DeGrado, *Acc. Chem. Res.* **2010**, *43*, 30–39.
[22] P. Claudon, A. Violette, K. Lamour, M. Decossas, S. Fournel, B. Heurtault, J. Godet, Y. Mély, B. Jamart-Grégoire, M.-C. Averlant-Petit, J.-P. Briand, G. Duportail, H. Monteil, G. Guichard, *Angew. Chem. Int. Ed.* **2010**, *49*, 333–336; *Angew. Chem.* **2010**, *122*, 343–346.
[23] A. Violette, S. Fournel, K. Lamour, B. Fischer, J.-P. Briand, H. Monteil, G. Guichard, *Chem. Biol.* **2006**, *13*, 531–538.
[24] C. Bonnel, B. Legrand, M. Simon, J. Martinez, J.-L. Bantignies, Y. K. Kang, E. Wenger, F. Hoh, N. Masurier, L. T. Maillard, *Chem. Eur. J.* **2017**, *23*, 17584–17591.
[25] M. M. Müller, M. A. Windsor, W. C. Pomerantz, S. H. Gellman, D. Hilvert, *Angew. Chem. Int. Ed.* **2009**, *48*, 922–925; *Angew. Chem.* **2009**, *121*, 940–943.
[26] F. D. Toste, M. S. Sigman, S. J. Miller, *Acc. Chem. Res.* **2017**, *50*, 609–615.
[27] D. Bécart, V. Diemer, A. Salaün, M. Oiarbide, Y. R. Nelli, B. Kauffmann, L. Fischer, C. Palomo, G. Guichard, *J. Am. Chem. Soc.* **2017**, *139*, 12524–12532.
[28] Z. C. Girvin, S. H. Gellman, *J. Am. Chem. Soc.* **2018**, *140*, 12476–12483.
[29] Z. C. Girvin, M. K. Andrews, X. Liu, S. H. Gellman, *Science* **2019**, *366*, 1528–1531.
[30] J. Aguesseau-Kondrotas, M. Simon, B. Legrand, J.-L. Bantigniès, Y. K. Kang, D. Dumitrescu, A. Van der Lee, J.-M. Campagne, R. M. de Figueiredo, L. T. Maillard, *Chem. Eur. J.* **2019**, *25*, 7396–7401.
[31] Z. C. Girvin, S. H. Gellman, *J. Am. Chem. Soc.* **2020**, *142*, 17211–17223.
[32] D. R. Holmes, C. W. Bunn, D. J. Smith, *J. Polym. Sci.* **1955**, *17*, 159–177.
[33] H. Arimoto, M. Ishibashi, M. Hirai, Y. Chatani, *J. Polym. Sci. Part A* **1965**, *3*, 317–326.
[34] S. Shima, H. Sakai, *Agric. Biol. Chem.* **1977**, *41*, 1807–1809.
[35] S. Shima, H. Matsuoka, T. Iwamoto, H. Sakai, *J. Antibiot.* **1984**, *37*, 1449–1455.
[36] B. Rodrigues, T. P. Morais, P. A. Zaini, C. S. Campos, H. O. Almeida-Souza, A. M. Dandekar, R. Nascimento, L. R. Goulart, *Sci. Rep.* **2020**, *10*, 11324.
[37] J. Lai, C. Zheng, D. Liang, Y. Huang, *Biomacromolecules* **2013**, *14*, 4515–4519.
[38] D. Huang, N. Korolev, K. D. Eom, J. P. Tam, L. Nordenskiöld, *Biomacromolecules* **2008**, *9*, 321–330.
[39] G. V. M. Sharma, B. S. Babu, D. Chatterjee, K. V. S. Ramakrishna, A. C. Kunwar, P. Schramm, H.-J. Hofmann, *J. Org. Chem.* **2009**, *74*, 6703–6713.
[40] M. Debnath, T. Das, D. Podder, D. Haldar, *ACS Omega* **2018**, *3*, 8760–8768.
[41] P. Papanek, J. E. Fischer, N. S. Murthy, *Macromolecules* **2002**, *35*, 4175–4182.
[42] C. Quarti, A. Milani, B. Civalleri, R. Orlando, C. Castiglioni, *J. Phys. Chem. B* **2012**, *116*, 8299–8311.
[43] S. Yamamoto, E. Ohnishi, H. Sato, H. Hoshina, D. Ishikawa, Y. Ozaki, *J. Phys. Chem. B* **2019**, *123*, 5368–5376.
[44] P. Schramm, H.-J. Hofmann, *THEOCHEM* **2009**, *907*, 109–114.
[45] B. Mennucci, R. Cammi, J. Tomasi, *J. Chem. Phys.* **1999**, *110*, 6858–6870.
[46] *GaussView*, Version 6.0, R. D., Dennington II, T. A. Keith, J. Millam, Gaussian, Inc., Wallingford, CT **2016**.
[47] *Gaussian 09,* Revision D.01, M. J. Frisch, G. W. Trucks, H. B. Schlegel, G. E. Scuseria, M. A. Robb, J. R. Cheeseman, G. Scalmani, V. Barone, B. Mennucci, G. A. Petersson, H. Nakatsuji, M. Caricato, X. Li, H. P. Hratchian, A. F. Izmaylov, J. Bloino, G. Zheng, J. L. Sonnenberg, M. Hada, M. Ehara, K. Toyota, R. Fukuda, J. Hasegawa, M. Ishida, T. Nakajima, Y. Honda, O. Kitao, H. Nakai, T. Vreven, J. A. Montgomery, Jr., J. E. Peralta, F. Ogliaro, M. Bearpark, J. J. Heyd, E. Brothers, K. N. Kudin, V. N. Staroverov, T. Keith, R. Kobayashi, J. Normand, K. Raghavachari, A. Rendell, J. C. Burant, S. S. Iyengar, J. Tomasi, M. Cossi, N. Rega, J. M. Millam, M. Klene, J. E. Knox, J. B. Cross, V. Bakken, C. Adamo, J. Jaramillo, R. Gomperts, R. E. Stratmann, O. Yazyev, A. J. Austin, R. Cammi, C. Pomelli, J. W. Ochterski, R. L. Martin, K. Morokuma, V. G. Zakrzewski, G. A. Voth, P. Salvador, J. J. Dannenberg, S. Dapprich, A. D. Daniels, O. Farkas, J. B. Foresman, J. V. Ortiz, J. Cioslowski, D. J. Fox, Gaussian, Inc., Wallingford, CT **2013**.
[48] Y. Zhao, D. G. Truhlar, *Theor. Chem. Acc.* **2008**, *120*, 215–241.
[49] Y. K. Kang, *THEOCHEM* **2001**, *546*, 183–193.
[50] W. J. Hehre, L. Radom, P. v. R. Schleyer, J. A. Pople, *Ab Initio Molecular Orbital Theory*, John Wiley & Sons, New York **1986**, Ch. 6.
[51] H. S. Park, Y. K. Kang, *New J. Chem.* **2019**, *43*, 17159–17173.
[52] *BIOVIA Discovery Studio*, Version 16, Dassault Systèmes Co., Waltham, Mass **2015**.
[53] P. Enkhbayar, S. Damdinsuren, M. Osaki, N. Matsushima, *Comput. Biol. Chem.* **2008**, *32*, 307–310.
[54] The PyMOL Molecular Graphics System, Version 2.6, Schrödinger, LLC.

Manuscript received: November 4, 2021
Revised manuscript received: December 21, 2021